Zwitterionic Biocompatible Quantum Dots for Wide pH Stability and Weak Nonspecific Binding to Cells

Vladimir V. Breus,[†,∥,*] Colin D. Heyes,[†,¶] Kyrylo Tron,[†] and G. Ulrich Nienhaus[†,‡,§,*]

[†]Institute of Biophysics, University of Ulm, Albert-Einstein-Allee 11, 89081 Ulm, Germany, [‡]Institute of Applied Physics and DFG-Center for Functional Nanostructures, University of Karlsruhe (TH), Wolfgang-Gaede-Strasse 1, 76131 Karlsruhe, Germany, and [§]Department of Physics, University of Illinois at Urbana—Champaign, Urbana, Illinois 61801. [∥]Present address: Institute of Physical Chemistry, University of Mainz, Jakob-Welder-Weg 11, 55099 Mainz, Germany. [¶]Present address: Department of Chemistry and Biochemistry, University of Arkansas, 345 N. Campus Drive, Fayetteville, Arkansas 72701.

ARTICLE

ABSTRACT Applications of water-soluble quantum dots (QDs) in the life sciences are limited by their poor colloidal stability in physiological media and nonspecific interaction with biomatter, particularly cell membranes. We have studied colloidal stability and nonspecific interactions with living cells for zwitterionic D-penicillamine-coated QDs (DPA-QDs) and the traditionally used carboxylated 11-mercaptoundecanoic acid-coated QDs (MUA-QDs) and found clear advantages of DPA-QDs. In single molecule fluorescence experiments, DPA-QDs showed no aggregation over the physiologically relevant pH range of 5—9, whereas MUA-QDs showed significant aggregation below pH 9. Upon exposure to living Mono Mac 6 cells, DPA-QDs, which possess overall charge-neutral surfaces, exhibited weak interactions with the cell membrane and were easily removed by flushing with buffer. By contrast, the highly charged MUA-QDs strongly associated with the cells and could not be removed even by extensive rinsing with buffer solution. DPA-QDs exhibit a high chemical stability even in strongly oxidizing conditions, in contrast to cysteine-coated QDs reported earlier. This beneficial property may arise from reduced interactions between DPA ligands due to steric effects of the methyl groups on their β-carbon atoms.

KEYWORDS: quantum dots · CdSe/ZnS · biocompatibility · aggregation · colloidal stability · cell imaging

Quantum dots (QDs) are promising fluorescent tools for many applications in the life sciences. They are bright, easily tunable in color, and extremely stable against photobleaching. However, each of the established approaches reported for water solubilization of QDs affects one or more essential properties required for optimal fluorescent biological labels, including small size, chemical stability, and fluorescence quantum yield. For cellular applications, the use of QDs coated with biocompatible ligands can be complicated by undesirable nonspecific interaction of the nanoparticles with cells.[1,2] Both the QD surface coating and the cell type influence the degree of nonspecific binding of nanocrystals.[3,4] Bare CdSe and CdTe QDs were reported to be acutely toxic for living cells since nanoparticle oxidation in biological environments leads to the release of Cd^{2+} ions.[1,5] However, adding a ZnS shell onto the fluorescent QD core, along with the increase in photoluminescence efficiency,[6,7] significantly reduces cytotoxicity,[1,5] as incubation of cells with core−shell QDs dispersed in culture medium showed no observable difference from untreated cells over a period of more than 2 weeks.[1,8−10] Injection of phospholipid-coated core−shell QDs into *Xenopus* embryos at a concentration of ~2 × 10^9 QDs/cell also revealed no toxicity as judged by their effect on the phenotype; the embryos developed normally up to late tadpole stages.[11] Interestingly, it was subsequently found that the effects of QDs on cells seem to depend on the cell type and the surface functionalization of the QDs.[12] Specifically, Hoshino *et al.*[13] reported that the toxic effect of QDs on biological objects may be significantly suppressed by a relatively dense and chemically stable ligand shell. More recently, QD functionalization has been shown to be important in biodistribution in animal models.[14−16] Mercaptocarboxylic acids are frequently used as ligands to obtain water-soluble fluorescence markers for studies of biological systems including cells. However, these QDs exhibit only limited solubility in buffers and cell culture media at neutral and acidic pH,[12,17,18] so that aggregation of the nanoparticles is frequently observed in solution or inside cells. This problem may be avoided by using thiolated, zwitterionic ligands, which contain both positively and negatively charged functional groups. We expect their colloidal stability to be higher because the ligands carry charges over a wide pH range, while the charge compensation at neutral pH should provide weaker nonspecific binding of the nanoparticles to

*Address correspondence to breus@uni-mainz.de, uli@uiuc.edu.

Received for review June 8, 2009 and accepted August 15, 2009.

Published online August 31, 2009. 10.1021/nn900600w CCC: $40.75

charged interfaces such as cell membranes. In a recent *in vivo* study, efficient renal clearance was shown for zwitterionic cysteine-coated QDs with hydrodynamic diameters <5.5 nm.[14] However, due to the spontaneous oxidation of the cysteine ligands, these nanoparticles aggregated within just a few hours after preparation and were stable only in the presence of reducing agents.[19]

D-Penicillamine (DPA, (2*S*)-2-amino-3-methyl-3-sulfanylbutanoic acid), a metabolite of penicillin, is a small trifunctional molecule used as a chelating agent. Unlike the mercaptoalkyl acids conventionally used for water solubilization of QDs, such as 11-mercaptoundecanoic acid (MUA), DPA is nontoxic and, in fact, even has pharmaceutical applications based on its ability to form chelates with heavy-metal ions, which enables their rapid renal excretion from the human body. D-Penicillamine has been applied in the treatment of copper metabolism disorders, cystinuria and mercury poisoning.[20] By exchanging the surfactants used during QD synthesis with DPA, its advantageous properties may be conferred to the resulting water-soluble QDs, yielding nanoparticles for life science applications, especially for *in vivo* experiments. In addition, DPA offers the opportunity for selective bioconjugation *via* its carboxylate group or its primary amino group. Once DPA is coordinated to the QD *via* its thiol group, DPA should maintain the overall charge neutrality of the particle. However, by simply blocking one of its functional groups, it should be possible to obtain negatively or positively charged (and monofunctional) nanoparticles as required.

The use of penicillamine enantiomers and its racemic mixture was recently reported by Moloney *et al.*[21] for the synthesis of chiral CdS QDs. However, the colloidal stability and cellular biocompatibility of DPA-coated QDs was not yet studied. Here we have investigated nonspecific interactions of different preparations of water-soluble QDs with Mono Mac 6 (MM6) cells. MM6 is a human monocytic cell line, isolated from the peripheral blood of a patient with monoblastic leukemia.[22] MM6 is the only established cell line that almost completely retains the phenotypic and functional features of mature monocytes, which are responsible for the ingestion of pathogens and foreign substances into the human body.[22] Therefore, we expected that QDs may be more efficiently internalized by MM6 cells than by other cell lines, but that zwitterionic QDs should display a higher resistance to interaction with the cells than those with highly charged and less stable coatings such as MUA-coated QDs. To test this hypothesis, we took a series of scanning confocal fluorescence microscopy images of MM6 cells which had been mixed with DPA-coated QDs (DPA-QDs) and MUA-coated QDs (MUA-QDs) at various concentrations.

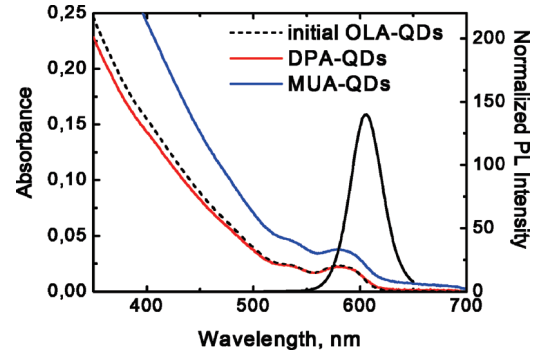

Figure 1. Absorption spectra of CdSe/ZnS QDs exchanged with DPA (red line), exchanged with MUA (blue line), and as-prepared in OLA (dotted black line). Solid black line represents the emission spectrum of the initial OLA-capped QDs.

RESULTS AND DISCUSSION

In order to prepare water-soluble QDs, initial surfactants such as oleylamine (OLA) were substituted by DPA or MUA by refluxing the nanoparticles in 2-propanol and dioxane/methanol cosolvent system,[23] respectively. Due to the low pK_a of the carboxylic acid group (1.8) and the relatively high pK_a of the amino group (7.9) in aqueous solution, DPA was only soluble in 2-propanol at pH > 10 when the amino group is deprotonated. Typically, a refluxing time of 10 min was sufficient for both ligands to replace the alkylamine surfactants of QDs, which is consistent with the results from Berrettini *et al.*[24] The absorption spectra of the resulting aqueous solutions of nanocrystals after exchange for 10, 25, 40, or 60 min were identical. Aqueous solutions of QDs that were reacted with DPA for 10−15 min demonstrated extremely high colloidal stability and showed no precipitation for at least 2−3 months. However, DPA-QDs exchanged for longer than 25−30 min usually precipitated within 2−3 weeks of storage in the dark. Alternatively, ligand substitution with DPA was performed by using a biphasic exchange method,[19] in which QDs dissolved in chloroform were mixed with DPA solution in PBS at pH 7.4 upon vigorous stirring at room temperature for 18 h. The resulting DPA-QDs showed identical behavior to the ones obtained by 10−15 min of refluxing in 2-propanol and did not precipitate from aqueous solution for at least several months. Therefore, flocculation of DPA-QDs exchanged for >30 min seems to result from too long exposure to refluxing conditions, resulting in possible side reactions involving amino and carboxylic groups of DPA ligands from different nanoparticles, with subsequent ligand dissociation from the QDs over a 2−3 week storage period. The resulting functionalized QDs retained about 40−60% of their initial photoluminescence efficiency.

In Figure 1, we compare the absorption spectra of aqueous DPA- and MUA-functionalized CdSe/ZnS QDs prepared from the same OLA-capped CdSe/ZnS stock with an overall quantum yield of 0.41. The absorption spectrum of MUA-QDs showed significant scattering

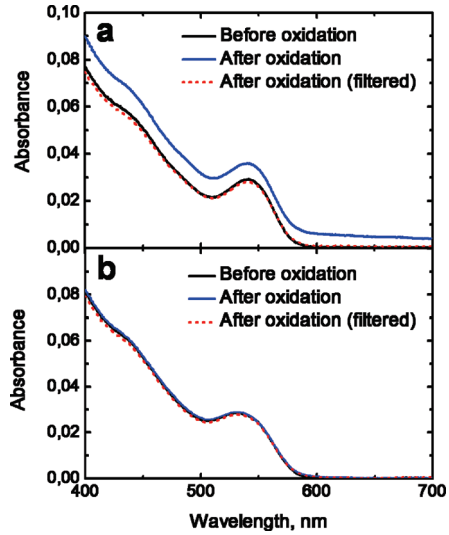

Figure 2. Absorption spectra of CdSe/ZnS QDs exchanged with DPA using (a) biphasic exchange and (b) refluxing methods, taken at three stages: before and after oxygen treatment for 1 h, and filtered through 0.2 μm membrane filter at the end of experiment.

due to partial aggregation of the QDs at near-neutral pH, which produces a sloping baseline underneath the spectrum, while the absorption spectrum of DPA-QDs showed no apparent aggregation.

Maintaining a basic pH during the exchange reaction was essential to avoid binding of amino and carboxyl groups of DPA to the surface of QDs along with or instead of the thiol group. Mercaptoamino acids are known to form polynuclear complexes with transition metal ions, for example, Zn(II)[25] and Cd(II),[26] involving two or more of their functional groups. For the pH range of 4−8, DPA-Cd polynuclear complexes of different stoichiometries have been reported, whereas in the basic pH region, mononuclear species prevail.[26] Overall, compared to cysteine, DPA is less likely to form polynuclear Zn(II) and Ni(II) complexes due to steric hindrance by the methyl groups of the β-carbon atom tending toward the metal ion.[25]

Steric constraints created by the methyl groups of DPA can also increase the resistance of DPA-QDs to aggregation induced by oxidative dimerization of thiol ligands reported for cysteine-coated QDs.[19] In contrast to our DPA-coated nanoparticles, cysteine-coated QDs tend to aggregate within a few hours after preparation. However, intense treatment of DPA-QD solutions, prepared by using the biphasic method, with dioxygen for 1 h induced the formation of small (<100 μm) nonfluorescent fiber-like white flakes, accompanied by a slight scattering background appearing in the absorbance spectrum of the sample (Figure 2a). Filtration through a 0.2 μm pore membrane resulted in virtually no reduction of the first absorption peak from its value before oxygen treatment (Figure 2a), suggesting that aggregated DPA rather than nanoparticles was present in the flocculate. The corresponding absorption spectra of

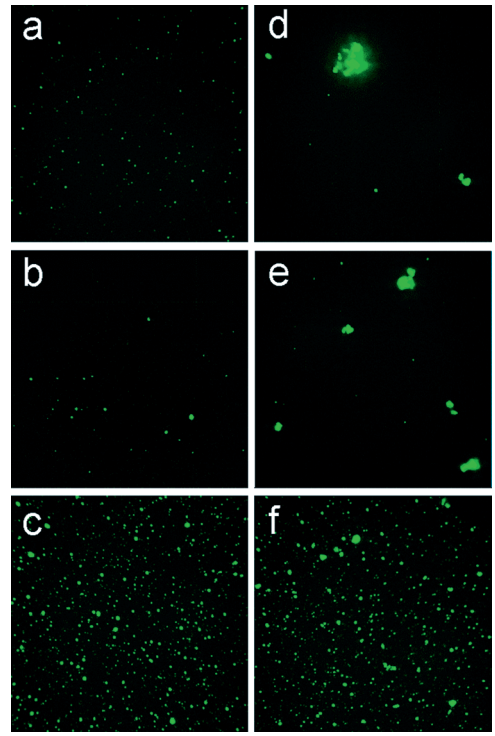

Figure 3. Colloidal stability of (a−c) DPA- and (d−f) MUA-functionalized quantum dots immobilized onto a poly-L-lysine-coated glass surface at pH 5.0 (a,d), 7.0 (b,e), and 9.2 (c,f).

the DPA-QDs prepared by using the refluxing approach are shown in Figure 2b. Interestingly, for this sample, changes in the absorption spectrum were absent before and after oxygen treatment, as well as after subsequent filtration (Figure 2b). Therefore, the slight oxidation effect, observed only for DPA-QDs exchanged using biphasic transfer at neutral pH, suggests that, along with the primary binding *via* thiol group, other functional groups of DPA bind to the QD surface at these conditions. Thereby, ligands arrange in a more irregular way, with methyl groups oriented away from the surface, exposing thiol groups for oxidative dimerization. However, even after treatment with oxygen, DPA-QDs prepared by using the biphasic approach were soluble for at least 2−3 weeks, in contrast to the untreated cysteine-coated QDs, which aggregated within a few hours after preparation.[19]

Figure 3 highlights the difference in colloidal stability between DPA-QDs and MUA-QDs at the single particle level in aqueous solution at different pH. These QDs were taken from the same stocks from which the spectra in Figure 1 were measured. For these experiments, we used a spinning disk confocal fluorescence microscope with laser excitation at 532 nm and detection by a sensitive EMCCD camera. In Figure 3a−c, typical fluorescence microscopy images of DPA-QDs immobilized on a poly-L-lysine-coated glass surface at pH 5.0, 7.0, and 9.2 are shown. Most of the spots were equal in size to the point spread function of the microscope for this wavelength (~0.3 μm) and were well-separated

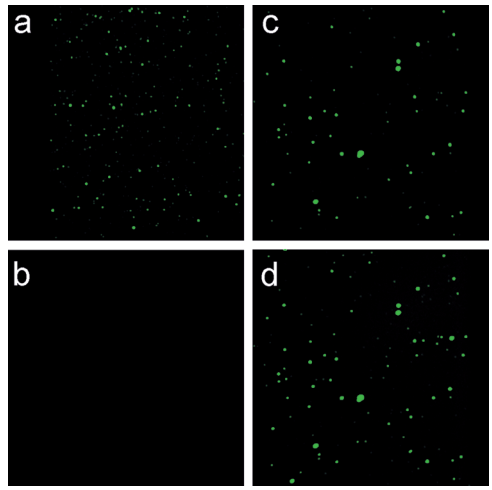

Figure 4. Water-soluble quantum dots deposited on plasma-cleaned glass surfaces: (a) 1 nM DPA-coated quantum dot solution added and (b) flushed with buffer, (c) 1 nM MUA-coated quantum dot solution added and (d) flushed with buffer. Each image is an average of 64 spinning disk fluorescence microscopy images.

and approximately equal in intensity, indicating that the DPA-QDs did not aggregate over the entire pH range studied. By contrast, images of MUA-QDs on the same surfaces showed significant aggregation at pH 5−7 (Figure 3d,e). Only at pH 9.2 (Figure 3f), the majority of MUA-QDs appeared nonaggregated and were more spatially dispersed. However, even at high pH, some small aggregates were still observed, probably as a result of the lower solubility of MUA in water compared to DPA. In a previous report by Reiss *et al.*,[27] ammonium hydroxide was added for the transfer of MUA-QDs into water after ligand exchange. Likewise, in the ligand exchange with dihydrolipoic acid, deprotonation of the resulting nanoparticles with potassium-*tert*-butoxide was reported to be a crucial step to achieve solubility in aqueous solution.[28] Thus, as Figure 3 shows, unlike MUA-QDs, DPA-coated nanoparticles did not aggregate over the important physiological pH range of 5−9.2.

Figure 4 demonstrates the nonspecific adsorption of 1 nM solutions of DPA-QD and MUA-QD samples to plasma-cleaned glass surfaces. Again, these samples were taken from the same stock as those characterized in Figure 1. DPA-QDs exposed to clean glass surfaces initially adhered to the glass as single, isolated particles but were easily removed upon flushing the surface with buffer solution (Figure 4a,b). In contrast, MUA-QDs (carrying a net charge and being partially aggregated) were strongly attracted to glass surfaces and were not washed away even after extensive flushing with buffer solution (Figure 4c,d). These results highlight the diversity in the adsorption forces of the differently functionalized QDs to charged surfaces.

Confocal fluorescence microscopy images illustrating the exposure of MM6 cells to 1 and 10 nM DPA- and MUA-QD solutions are shown in Figure 5. Those QDs were also prepared from the same OLA-coated CdSe/ZnS stock as those on which the data in Figure 1 were taken and had the same size (d = 6.2 nm) and emission maximum at 606 nm. In each experiment, MM6 cells, adhered to the surface of the glass slide of a sample chamber, were exposed to 1 nM QD solution for 60 min. Then, the samples were rinsed several times with fresh buffer. Subsequently, a 10 nM QD solution was introduced for a further 60 min of exposure. Following this step, the samples were rinsed with buffer and, finally, propidium iodide (PI) solution was added at the end of the experiment in order to test cell viability.[29] At 1 nM concentration, a very slight, nonspecific interaction between the DPA-QDs and the cell membrane was observed (Figure 5b). Upon flushing with buffer, practically all DPA-QDs were removed from the cell membrane (Figure 5c). At 10 nM concentration, significant nonspecific interaction of the DPA-QDs with the cell

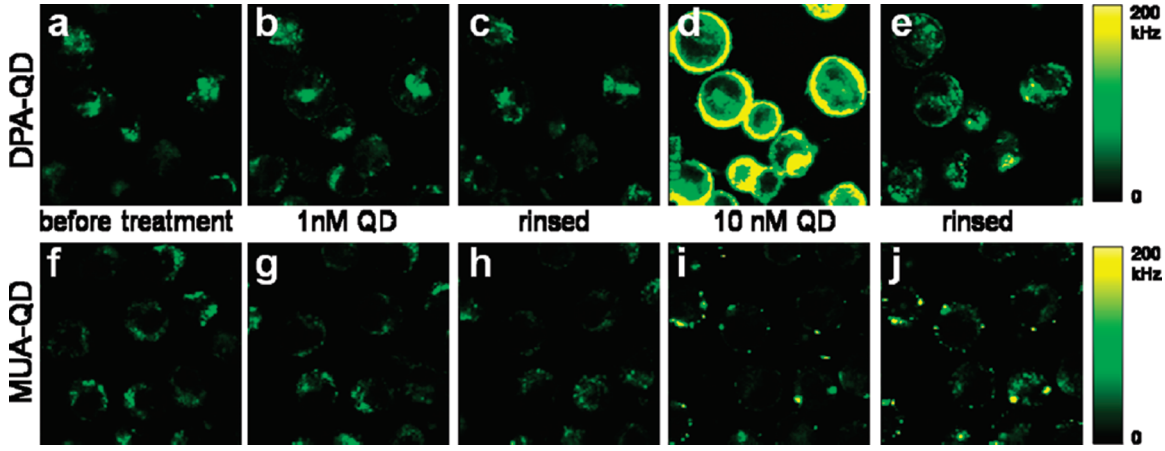

Figure 5. (a−e) Sequential images of MM6 cells at pH 7.4 with DPA-QDs: (a) before addition of DPA-QDs (showing cellular autofluorescence), (b) after 60 min of exposure to 1 nM DPA-QD solution, (c) after thorough rinsing with buffer, (d) after 60 min of interaction with 10 nM DPA-QD solution, and (e) rinsing at the end of the experiment. (f−j) Sequential images of MM6 cells at pH 7.4 with MUA-QDs: (f) before addition of MUA-QDs (showing cellular autofluorescence), (g) after 60 min of exposure to 1 nM MUA-QD solution, (h) after thorough rinsing with buffer, (i) after 60 min of interaction with 10 nM MUA-QD solution, and (j) rinsing at the end of the experiment.

membrane appeared as a homogeneous fluorescence ring (Figure 5d). Again, after rinsing with buffer, the QDs were almost completely washed away from the cell, leaving only a small fraction still attached to the membrane (Figure 5e). Nuclear staining was absent after addition of PI at the end of the experiment, indicating that the cells were still alive and well and, specifically, had intact membranes. Consequently, the QDs were not harmful to the cells at these concentrations, at which they are commonly used for fluorescence labeling.

The corresponding images of MM6 cells upon exposure to MUA-QD solutions are shown in Figure 5f−j. For MUA-QDs, a very different behavior is observed. At 1 nM concentration, the QDs did not attach to the cells during 1 h of exposure (Figure 5g), while at 10 nM, the MUA-QDs attached to the cellular membrane as aggregates, staining them inhomogeneously (Figure 5i). Flushing the cells with clean buffer did not remove the QD aggregates from the cell membranes (Figure 5j). Such a strong nonspecific binding is disadvantageous when using MUA-QDs for cellular labeling.

The concentrations of both MUA-QDs and DPA-QDs quoted here for our experiments were derived from the absorption spectra of bulk solutions, using an empirical formula that relates the QD size to the molar absorptivity, ε.[30] However, since MUA-QDs were partially aggregated at neutral pH, the number of individual MUA-QD entities present at pH 7.4 was much reduced compared to DPA-QDs. Additionally, the molar extinction coefficient determination is likely affected by aggregation, further complicating the accurate determination of the MUA-QD concentration. In order to more accurately estimate the effective concentration of dispersed MUA-QDs in the solution, we positioned the focus of the scanning confocal microscope into the solution above the cells and collected fluorescence time traces (Figure 6a). From these traces, photon counting histograms (PCH)[31,32] were assembled to determine the aggregation state of the QDs (Figure 6b). If completely dispersed, a 1 nM concentration will give only one QD on average within the ~1 fl confocal volume of the microscope at any given time, each with an intensity of about 8−10 counts/ms at the laser power (1 μW) used, which is also the typical intensity observed for individual, surface-immobilized QDs.[33] Consequently, an average intensity of about 80−100 counts/ms is expected for 10 nM QD concentration. However, PCH analysis yielded a most probable intensity of 20−30 counts/ms for 10 nM MUA-QD solutions in PBS at pH 7.4, which is much smaller than expected (Figure 6b). The elongated tail at higher count rates in the PCH as well as the presence of sharp, intense spikes in the fluorescence traces indicated the presence of aggregates in 10 nM MUA-QD solution. In contrast, DPA-QDs showed a constant intensity even at 50 nM, with no spikes visible over the whole 60 s trace (Figure 6a,b).

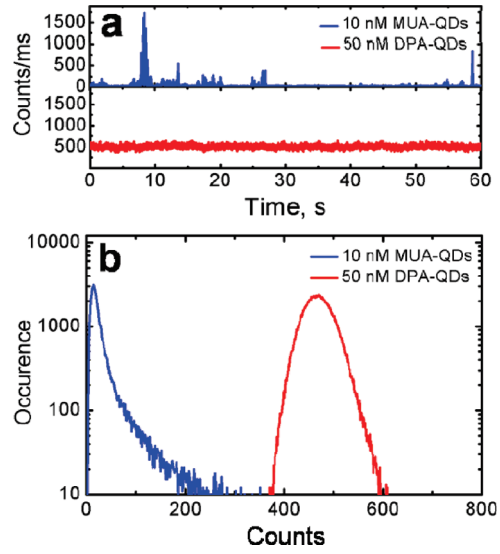

Figure 6. (a) Fluorescence traces of solutions of DPA-coated QDs (50 nM) and MUA-coated QDs (10 nM) and (b) the corresponding photon counting histograms.

For DPA-QDs at 50 nM concentration, the most probable intensity was approximately 450−500 counts/ms (Figure 6b). This intensity is 50-fold that expected for a 1 nM solution, suggesting the presence of nonaggregated QDs. Aggregation also explains the lower fluorescence intensity of MUA-QDs relative to the DPA-QDs on the surfaces of MM6 cells (Figure 5b). At both 1 and 10 nM MUA-QD concentrations, a considerable fraction of aggregated MUA-QDs is present, which effectively reduces the number of MUA-QD species in solution that are capable of interacting with the cell membrane. In any case, the ease with which DPA-QDs can be washed away from the cell membrane relative to MUA-QDs suggests that DPA-QDs rather than MUA-QDs should be highly preferable for specific labeling in cellular imaging.

To determine the fate of QDs that did interact with the cells, we analyzed the confocal images shown in Figure 5 as follows. For each cell, the fluorescence intensity was integrated over the entire cell (circular area with diameter d_1) and also over the interior region (circular area with diameter $0.75 \times d_1$) to estimate QD uptake by the cell. Figure 7 shows the average fluorescence intensity of a cell, separated into contributions from the membrane and the cellular interior. For both DPA- and MUA-QD, the data in Figure 7a,b represent the analysis of the confocal images that were shown in Figure 5a−e and f−j, respectively.

For 1 nM DPA-QDs, the slight increase in the overall intensity of the cell upon addition of QDs appears to arise primarily from membrane−QD interactions and was effectively removed by rinsing (Figure 7a). No significant increase in the fluorescence from the cell interior was found following 60 min of exposure or after rinsing with buffer (Figure 7a). The addition of 1 nM MUA-QD solution to MM6 cells did not cause any de-

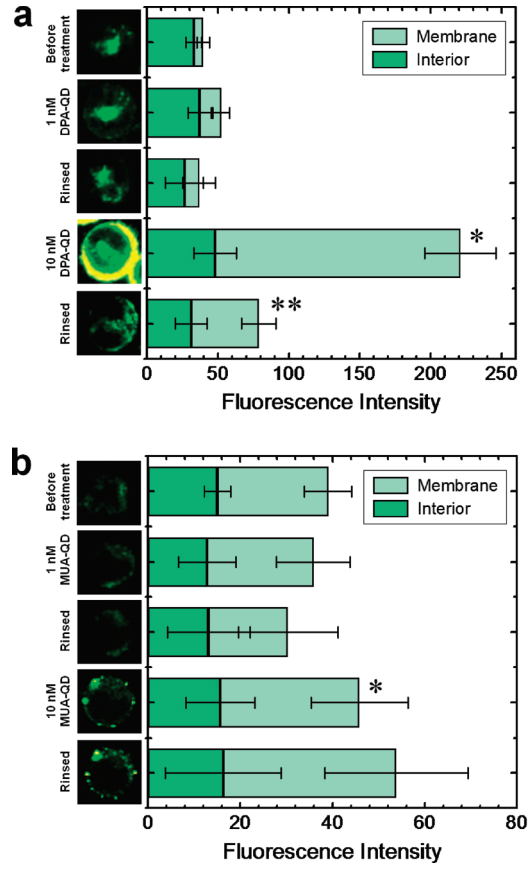

Figure 7. Nonspecific interaction of MM6 cells with (a) DPA-QDs and (b) MUA-QDs. Columns represent integrated fluorescence intensity from corresponding confocal scans shown in Figure 5, averaged over several cells with contributions from the edges (plasma membrane) and the interior (cytoplasm and organelles) of the cell in light and dark green, respectively. The intensity was calculated for the autofluorescence of MM6 cells before the addition of QDs, after 60 min of interaction with 1 nM QD solution, after thorough rinsing of the channel with buffer, after 60 min of interaction with 10 nM QD solution, and after final rinsing at the end of the experiment. Significant difference, $p < 0.05$: * treatment with 10 nM QD solution *vs* first rinsing; ** second rinsing *vs* treatment with 10 nM QD solution.

tectable fluorescence increase either inside the cell or on the cellular membrane (Figure 7b). This result is probably due to the reduced effective concentration of interacting species in solution caused by aggregation, as discussed above. The decrease in the intracellular fluorescence over time (Figure 7b) likely arises from photobleaching of naturally occurring fluorophores in the cell that produce the autofluorescence observed in nontreated cells (Figure 5a,f).

Upon exposure of MM6 cells to 10 nM DPA-QDs, the overall fluorescence intensity increased by 5−6-fold, mostly from an increase in the membrane-associated fluorescence, along with a slight increase in the cell interior, which was found in several cells (Figure 6a). After flushing, about 80−85% of the DPA-QDs were washed off of the membrane, whereas for 10 nM MUA-QDs, the amount of QDs both bound to the membrane and penetrated inside the cell continuously increased over the 1 h period of exposure. The fluorescence could not be reduced by flushing (Figure 6b) due to the fact that MUA-QDs were more strongly associated with the cell membrane. This increased attraction relative to DPA-QDs may result from strong electrostatic interactions between the highly negatively charged MUA-QDs and the charged phospholipid headgroups of the membrane lipids, similar to the way that MUA-QDs interact strongly with bare glass surfaces (Figure 4) and/or hydrophobic interactions between the long hydrocarbon MUA chains on the MUA-QDs (which is absent in DPA-QDs) and the hydrophobic domains of the lipids within the membrane.

SUMMARY AND CONCLUSIONS

Compared with cysteine-coated nanoparticles reported earlier,[14,19] DPA-QDs showed higher chemical stability and resistance to oxidation. The presence of both positively and negatively charged functional groups on the DPA-QD surface results in a high solubility in water over a wide pH range compared to the more commonly used carboxylic acid-functionalized QDs. For MUA-QDs at pH close to neutral, the carboxylic acid groups on the surface were only partially deprotonated. Even at high pH, the deprotonated MUA-QDs showed some aggregation tendency. However, due to the large negative surface charge of MUA-QDs, strong attraction of MUA-QDs to both plasma-cleaned glass slides and MM6 cells was observed. DPA-QDs also interacted with MM6 cells but were easily removed by flushing with buffer, so we can conclude that this interaction is rather weak compared to MUA-QDs. Long exposure of the cells to high concentrations of DPA-QDs (~10 nM) allowed some of the nanoparticles to penetrate the plasma membrane and enter the interior of the cell. However, even when this small amount of DPA-QDs penetrated into the cellular interior, the vast majority of cells were viable, suggesting no toxic effects of the nanoparticles upon interaction with cells at up to 10 nM concentration on the 2 h time scale. This result indicates that intracellular labeling with DPA-QDs appears very promising.

Labeling of cells with functionalized, bioconjugated QDs has certain limitations, such as nonspecific binding of the particles to the cells. At low concentrations (*e.g.*, those used for single particle tracking experiments), one must be certain that the label is specifically bound to the biomolecule of interest, while at high concentrations, nonspecific binding will increase the overall fluorescence background. The lack of aggregation, confirmed by PCH, and low nonspecific binding of DPA-QDs, observed by confocal microscopy, suggests that they will be excellent for use in cell-based assays. Resistance to oxidation and colloidal stability of DPA-QDs over a wide pH range are useful for specific labeling inside the cell, where the pH may vary from neutral

to acidic, depending on the cellular compartment of interest. Therefore, strategies of bioconjugation of DPA-QDs to proteins and antibodies should be further developed.

METHODS

Materials: All chemicals were purchased from Sigma Aldrich (Taufkirchen, Germany), and the highest purity grade available was used.

Synthesis of CdSe/ZnS Core/Shell QDs: The synthesis of CdSe nanoparticles was based on a combination of the methods from Murray and Bawendi,[34] Talapin *et al.*,[6] and Peng and Peng.[35] Briefly, CdO (0.80 mmol) and stearic acid (4.22 mmol) were heated to 200−250 °C under an argon atmosphere until a clear, colorless solution was obtained. Trioctylphosphine oxide (TOPO) (8.66 mmol) and hexadecylamine (HDA) (6.83 mmol) were added to the reaction mixture, and the temperature was further increased to 300 °C. At this temperature, heating was removed and a solution of Se (0.80 mmol) in 4 mL of trioctylphosphine (TOP) was quickly injected into the reaction mixture under vigorous stirring, which led to immediate nucleation and growth of the nanoparticles. Aliquots were taken at 1−3 min time intervals and dispersed in cold toluene.

In a typical overcoating reaction, to the calculated amount of CdSe QDs toluene solution, 6 mL of oleylamine (OLA) and 2 mL of oleic acid (OA) were added, and the mixture was degassed at room temperature for 30 min to evaporate the toluene. Thereafter, the system was switched to argon atmosphere and the temperature was increased to 165 °C, at which the amounts of 0.2 M sulfur and zinc injection solutions, corresponding to one monolayer of ZnS, were introduced in an alternating manner (SILAR)[36] with 15 min itervals by slow dripping. After the desired amount of monolayers was achieved, the reaction was stopped, the solution cooled to room temperature, and the product separated from the unreacted precursors by precipitation of the particles in a methanol−hexane solution and centrifugation at 10416*g* for 1 h. The zinc injection solution was prepared by dissolving zinc stearate in a 1:5 mixture of OA and OLA at 100 °C. The sulfur injection solution was prepared separately by dissolving elemental sulfur in OLA at room temperature.

Surface Ligand Exchange with MUA and DPA: The exchange reaction was performed as reported earlier:[23] 120 mg of MUA (or 80 mg of DPA) was dissolved in 30 mL of a 1:1 (v/v) methanol/dioxane solvent (30 mL of 2-propanol for functionalization with DPA), and the pH of the solution was adjusted to 12−13 with tetramethylammonium hydroxide pentahydrate (TMAHP). In case of ligand exchange with DPA, the mixture was sonicated for 1−2 min to obtain a clear solution. Then, 20 nmol of OLA-coated CdSe/ZnS QDs was added, and the temperature was increased to 70−80 °C while stirring under nitrogen atmosphere. After 15−20 min of refluxing, the mixture was cooled to room temperature. The exchanged particles were precipitated with ethyl acetate. The solution was centrifuged at 10 416*g* for 45 min, and the resulting pellet was redissolved in 18.2 MΩ · cm Millipore water.

The biphasic ligand exchange of DPA was performed according to Liu *et al.*[19] To a solution of DPA (50 mg) in 2.5 mL phosphate buffered saline (PBS, pH 7.4) was added 10 nmol of OLA-coated CdSe/ZnS QDs dissolved in 2.5 mL of chloroform. After vigorous stirring of these two phases for ~18 h, the nearly colorless chloroform phase was removed with a pipet, and the rest of the organic content was evaporated under reduced pressure. The QDs were then precipitated with ethanol, centrifuged, and redispersed in PBS buffer.

Oxidation Resistance Test: The absorption spectra of PBS (pH 7.4) solutions of DPA-QDs, obtained using different ligand exchange methods, were measured before and after bubbling an intense oxygen flow through the solutions at room temperature for 1 h. The QD solutions were then purged through 0.2 μm membrane filters, and the absorption spectra were remeasured.

Fluorescence Microscopy Experiments: We used a home-built scanning confocal fluorescence microscope[37,38] with Ar^+ ion laser excitation at 514 nm (1 μW) and detection by an avalanche photodiode detector for the studies of nonspecific interaction of water-soluble QDs to cells, and a spinning disk confocal fluorescence microscope, equipped with a Yokogawa CSU 10 spinning disk unit, a 532-nm Nd:YAG excitation laser and an Andor iXon DV887 ECS-BV EMCCD camera, for the investigation of colloidal stability of water-soluble QD preparations. The emission from the QDs was detected using a 582/50 nm band-pass for scanning confocal and a 585/80 nm band-pass for spinning disk fluorescence microscopy experiments, respectively.

Colloidal Stability of Water-Soluble CdSe/ZnS QDs: Solutions (10 nM) of MUA-CdSe/ZnS and DPA-CdSe/ZnS QDs at different pH were prepared from 1 μM stock solutions by dissolving 10 μL of QDs in 990 μL of the corresponding buffer. They were kept in buffer for about 24 h for equilibration prior to the measurements. The following buffers were used: pH 5.0, 100 mM sodium citrate/sodium phosphate buffer; pH 7.0, 100 mM sodium phosphate buffer; and pH 9.2, 100 mM sodium carbonate buffer. Water-soluble QDs were immobilized on poly-L-lysine-coated plasma-cleaned glass slides of a sandwich sample cell, which consisted of a 20 × 20 mm^2 glass slide (Menzel-Gläser, Braunschweig, Germany) attached to a 24 × 32 mm^2 glass slide (Menzel-Gläser, Braunschweig, Germany) with two strips of ~200 μm double-sided adhesive tape, forming a ~3−4 mm wide channel between the upper and lower glass slides. To coat the glass slides was added 20 μL of 0.01% poly-L-lysine in 100 mM PBS (pH 7.4) into a channel, formed by two glass coverslips and double-sided adhesive tape, and left to react with the glass surface for 15−20 min. Then the channel was flushed with 18.2 MΩ · cm Millipore water several times. Twenty microliters of QDs in buffer was added to the channel and left for another 15−20 min. Subsequently, the channel was rinsed several times with the corresponding buffer.

Nonspecific Interactions of QDs with Cells: Human monocytic cell line Mono Mac 6 (MM6) was obtained from the German Collection of Microorganisms and Cell Cultures (DSMZ, Braunschweig, Germany). The cells were cultured in suspension in advanced RPMI 1640 medium (Invitrogen) supplemented with 10% fetal calf serum (FCS) and 1% penicillin/streptomycin/L-glutamine (PSG). The cells were sedimented prior to experiments, transferred to PBS (pH 7.4), and introduced into the channel of the sandwich sample cell (omitting poly-L-lysine coating). After waiting 20 min for the cells to adhere to the surface of the bottom glass slide, the channel was rinsed with fresh portions of buffer to remove non-adhering cells. Afterward, solutions containing the appropriate concentrations of water-soluble QDs in PBS (pH 7.4) were filled into the channel of the sandwich. To ensure cell viability during and after completion of confocal fluorescence microscopy experiments, we added 75 nmol/L PI (Molecular Probes, Eugene, OR), which cannot penetrate into the cells as long as they are viable. As a positive control, subsequent permeabilization with 0.1% Triton X-100 (Sigma-Aldrich, Taufkirchen, Germany) yielded bright nuclear staining due to the integration of PI into nuclear DNA. All cell-based experiments were performed at room temperature (~25 °C).

Statistical Analysis: Integrated fluorescence intensity data from confocal scans of MM6 cells interacting with QDs are presented as mean ± standard deviation (SD). Statistical comparisons of fluorescence intensity differences were performed using paired Student's *t*-test (Origin 6.1, OriginLab Corporation, Northampton, MA), and *p* values of less than 0.05 were considered significant.

Acknowledgment. We acknowledge support by the Deutsche Forschungsgemeinschaft (DFG) and the State of Baden-Württemberg through the DFG-Center for Functional Nanostructures (CFN) and by DFG Grants Ni291/7 and Ni291/8, SFB497.

REFERENCES AND NOTES

1. Derfus, A. M.; Chan, W. C. W.; Bhatia, S. N. Probing the Cytotoxicity of Semiconductor Quantum Dots. *Nano Lett.* **2004**, *4*, 11–18.

2. Michalet, X.; Pinaud, F. F.; Bentolila, L. A.; Tsay, J. M.; Doose, S.; Li, J. J.; Sundaresan, G.; Wu, A. M.; Gambhir, S. S.; Weiss, S. Quantum Dots for Live Cells and *In Vivo* Imaging and Diagnostics. *Science* **2005**, *307*, 538–544.
3. Bentzen, E. L.; Tomlinson, I. D.; Mason, J.; Gresch, P.; Warnement, M. R.; Wright, D.; Sanders-Bush, E.; Blakely, R.; Rosenthal, S. J. Surface Modification to Reduce Nonspecific Binding of Quantum Dots in Live Cell Assays. *Bioconjugate Chem.* **2005**, *16*, 1488–1494.
4. Kairdolf, B. A.; Mancini, M. C.; Smith, A. M.; Nie, S. Minimizing Nonspecific Cellular Binding of Quantum Dots with Hydroxyl-Derivatized Surface Coatings. *Anal. Chem.* **2008**, *80*, 3029–3034.
5. Cho, S. J.; Maysinger, D.; Jain, M.; Roder, B.; Hackbarth, S.; Winnik, F. M. Long-Term Exposure to CdTe Quantum Dots Causes Functional Impairments in Live Cells. *Langmuir* **2007**, *23*, 1974–1980.
6. Talapin, D. V.; Rogach, A. L.; Kornowski, A.; Haase, M.; Weller, H. Highly Luminescent Monodisperse CdSe and CdSe/ZnS Nanocrystals Synthesized in a Hexadecylamine-Trioctylphosphine Oxide-Trioctylphospine Mixture. *Nano Lett.* **2001**, *1*, 207–211.
7. Heyes, C. D.; Kobitski, A. Y.; Breus, V. V.; Nienhaus, G. U. Effect of the Shell Thickness on the Blinking Statistics of Core−Shell Quantum Dots: A Single-Particle Fluorescence Study. *Phys. Rev. B* **2007**, *75*, 1254311–1254318.
8. Jaiswal, J. K.; Mattoussi, H.; Mauro, J. M.; Simon, S. M. Long-Term Multiple Color Imaging of Live Cells Using Quantum Dot Bioconjugates. *Nat. Biotechnol.* **2003**, *21*, 47–51.
9. Parak, W. J.; Boudreau, R.; Gros, M. L.; Gerion, D.; Zanchet, D.; Micheel, C. M.; Williams, S. C.; Alivisatos, A. P.; Larabell, C. Cell Motility and Metastatic Potential Studies Based on Quantum Dots Imaging of Phagokinetic Tracks. *Adv. Mater.* **2002**, *14*, 882–885.
10. Pinaud, F.; King, D.; Moore, H.-P.; Weiss, S. Bioactivation and Cell Targeting of Semiconductor CdSe/ZnS Nanocrystals with Phytochelatin-Related Peptides. *J. Am. Chem. Soc.* **2004**, *126*, 6115–6123.
11. Dubertret, B.; Skourides, P.; Norris, D. J.; Noireaux, V.; Brivanlou, A. H.; Libchaber, A. *In Vivo*Imaging of Quantum Dots Encapsulated in Phospholipid Micelles. *Science* **2002**, *298*, 1759–1762.
12. Parak, W. J.; Pellegrino, T.; Plank, C. Labelling of Cells with Quantum Dots. *Nanotechnology* **2005**, *16*, R9–R25.
13. Hoshino, A.; Fujioka, K.; Oku, T.; Suga, M.; Sasaki, Y. F.; Ohta, T.; Yasuhara, M.; Suzuki, K.; Yamamoto, K. Physicochemical Properties and Cellular Toxicity of Nanocrystal Quantum Dots Depend on Their Surface Modification. *Nano Lett.* **2004**, *4*, 2163–2169.
14. Choi, H. S.; Liu, W.; Misra, P.; Tanaka, E.; Zimmer, J. P.; Itty Ipe, B.; Bawendi, M. G.; Frangioni, J. V. Renal Clearance of Quantum Dots. *Nat. Biotechnol.* **2007**, *25*, 1165–1170.
15. Daou, T. J.; Li, L.; Reiss, P.; Josserand, V.; Texier, I. Effect of Poly(ethylene glycol) Length on the *In Vivo* Behavior of Coated Quantum Dots. *Langmuir* **2009**, *25*, 3040–3044.
16. Li, L.; Daou, T. J.; Texier, I.; Chi, T. T. K.; Liem, N. Q.; Reiss, P. Highly Luminescent $CuInS_2$/ZnS Core/Shell Nanocrystals: Cadmium-Free Quantum Dots for *In Vivo* Imaging. *Chem. Mater.* **2009**, *21*, 2422–2429.
17. Aldana, J.; Lavelle, N.; Wang, Y.; Peng, X. Size-Dependent Dissociation pH of Thiolate Ligands from Cadmium Chalcogenide Nanocrystals. *J. Am. Chem. Soc.* **2005**, *127*, 2496–2504.
18. Algar, W. R.; Krull, U. J. Luminescence and Stability of Aqueous Thioalkyl Acid Capped CdSe/ZnS Quantum Dots Correlated to Ligand Ionization. *ChemPhysChem* **2007**, *8*, 561–568.
19. Liu, W.; Choi, H. S.; Zimmer, J. P.; Tanaka, E.; Frangioni, J. V.; Bawendi, M. G. Compact Cysteine-Coated CdSe(ZnCdS) Quantum Dots for *In Vivo* Applications. *J. Am. Chem. Soc.* **2007**, *129*, 14530–14531.
20. Weigert, W. M.; Offermanns, H.; Scherberich, P. D-Penicillamine—Production and Properties. *Angew. Chem., Int. Ed. Engl.* **1975**, *14*, 330–336.
21. Moloney, M. P.; Gun'ko, Y. K.; Kelly, J. M. Chiral Highly Luminescent CdS Quantum Dots. *Chem. Commun.* **2007**, *38*, 3900–3902.
22. Ziegler-Heitbroc, H. W. L.; Thiel, E.; Futterer; Herzog, V.; Wirtz, A.; Riethmuller, G. Establishment of a Human Cell Line (Mono Mac 6) with Characteristics of Mature Monocytes. *Int. J. Cancer* **1988**, *41*, 456–461.
23. Breus, V. V.; Heyes, C. D.; Nienhaus, G. U. Quenching of CdSe−ZnS Core−Shell Quantum Dot Luminescence by Water-Soluble Thiolated Ligands. *J. Phys. Chem. C* **2007**, *111*, 18589–18594.
24. Berrettini, M. G.; Braun, G.; Hu, J. G.; Strouse, G. F. NMR Analysis of Surface and Interfaces in 2-nm CdSe. *J. Am. Chem. Soc.* **2004**, *126*, 7063–7070.
25. Sovago, I.; Gergely, A.; Harman, B.; Kiss, T. Complexes of Sulphur-Containing Ligands-II: Binary and Ternary Complexes of D-Penicillamine and L-Cysteine with Nickel(II) and Zinc(II) Ions. *J. Inorg. Nucl. Chem.* **1979**, *41*, 1629–1633.
26. Avdeef, A.; Kearney, D. L. Cadmium Binding by Biological Ligands. 1. Formation of Protonated Polynuclear Complexes between Cadmium and D-Penicillamine in Aqueous Solution. *J. Am. Chem. Soc.* **1982**, *104*, 7212–7218.
27. Reiss, P.; Bleuse, J.; Pron, A. Highly Luminescent CdSe/ZnSe Core/Shell Nanocrystals of Low Size Dispersion. *Nano Lett.* **2002**, *2*, 781–784.
28. Mattoussi, H.; Mauro, J. M.; Goldman, E. R.; Anderson, G. P.; Sundar, V. C.; Mikulec, F. V.; Bawendi, M. G. Self-Assembly of CdSe−ZnS Quantum Dot Bioconjugates Using an Engineered Recombinant Protein. *J. Am. Chem. Soc.* **2000**, *122*, 12142–12150.
29. Röcker, C.; Manolov, D. E.; Kuzmenkina, E. V.; Tron, K.; Slatosch, H.; Torzewski, J.; Nienhaus, G. U. Affinity of C-Reactive Protein toward FcgRI Is Strongly Enhanced by the g-Chain. *Am. J. Pathol.* **2007**, *170*, 755–763.
30. Yu, W. W.; Qu, L.; Guo, W.; Peng, X. Experimental Determination of the Extinction Coefficient of CdTe and CdSe and CdS Nanocrystals. *Chem. Mater.* **2003**, *15*, 2854–2860.
31. Chen, Y.; Muller, J. D.; So, P. T.; Gratton, E. The Photon Counting Histogram in Fluorescence Fluctuation Spectroscopy. *Biophys. J.* **1999**, *77*, 553–567.
32. Zemanová, L.; Schenk, A.; Hunt, N.; Nienhaus, G. U.; Heilker, R. Endothelin Receptor in Virus-like Particles: Ligand Binding Observed by Fluorescence Fluctuation Spectroscopy. *Biochemistry* **2004**, *43*, 9021–9028.
33. Owen, R. J.; Heyes, C. D.; Knebel, D.; Röcker, C.; Nienhaus, G. U. An Integrated Instrumental Setup for the Combination of Atomic Force Microscopy with Optical Spectroscopy. *Biopolymers* **2006**, *82*, 410–414.
34. Murray, C. B.; Norris, D. J.; Bawendi, M. G. Synthesis and Characterization of Nearly Monodisperse CdE (E = S and Se and Te) Semiconductor Nanocrystallites. *J. Am. Chem. Soc.* **1993**, *115*, 8706–8715.
35. Peng, Z. A.; Peng, X. Formation of High-Quality CdTe and CdSe and CdS Nanocrystals Using CdO as Precursor. *J. Am. Chem. Soc.* **2001**, *123*, 183–184.
36. Li, J. J.; Wang, Y. A.; Guo, W.; Keay, J. C.; Mishima, T. D.; Johnson, M. B.; Peng, X. Large-Scale Synthesis of Nearly Monodisperse CdSe/CdS Core/Shell Nanocrystals Using Air-Stable Reagents *via* Successive Ion Layer Adsorption and Reaction. *J. Am. Chem. Soc.* **2003**, *125*, 12567–12575.
37. Heyes, C. D.; Kobitski, A. Y.; Amirgoulova, E. V.; Nienhaus, G. U. Biocompatible Surfaces for Specific Tethering of Individual Protein Molecules. *J. Phys. Chem. B* **2004**, *108*, 13387–13394.
38. Schenk, A.; Ivanchenko, S.; Röcker, C.; Wiedenmann, J.; Nienhaus, G. U. Photodynamics of Red Fluorescent Proteins Studied by Fluorescence Correlation Spectroscopy. *Biophys. J.* **2004**, *86*, 384–394.